GROUND-BASED REMOTE SENSING PROFILING OF AEROSOLS, BOUNDARY LAYER AND LIQUID WATER CLOUDS USING SYNERGISTIC RETRIEVALS

G. Martucci [(1)], A. Chauvigne [(2)], E.J. O'Connor [(3),(4)], A. Hirsikko [(3)], D. Ceburnis[(1)], W. Wobrock[(2)], C. D. O'Dowd[(1)]

[(1)] *School of Physics & Centre for Climate and Air Pollution Studies, Ryan Institute, National University of Ireland Galway, University Road, Galway, Ireland*

[(2)] *Clermont Université, Université Blaise Pascal, Laboratoire de Météorologie Physique, F-63000 Clermont-Ferrand, France*

[(3)] *Finnish Meteorological Institute, P.O. BOX 503, FI-00101, Helsinki, Finland*

[(4)] *Univ. Reading, Reading, Berks, England*

ABSTRACT

Multiple techniques based on synergistic ground-based remote sensing instrumentation to retrieve the vertical structure of the atmospheric boundary layer (ABL), the aerosol mass concentration from the LIDAR extinction and the liquid cloud microphysics are presented. The vertical structure of the ABL during day and night is retrieved by applying the Temporal Height Tracking algorithm to the backscatter and Doppler velocity LIDAR profiles; the calculation of the extinction coefficient from LIDAR returns in combination with in-situ aerosol measurements allow the characterization and categorization of different aerosol layers as well as the estimate of the aerosol mass concentration profile; the SYRSOC (SYnergistic Remote Sensing Of Cloud) technique [1,2,3] utilises a K_a-band Doppler cloud RADAR, a single-channel LIDAR and a multichannel microwave-radiometer to retrieve the main microphysical parameters such as cloud droplet number concentration (CDNC), droplets effective radius (R_{eff}), cloud liquid water content (LWC), cloud optical thickness, cloud Albedo and cloud LIDAR multiple scattering. Three comparisons are presented to validate the retrieved microphysics: between surface-sampled cloud condensation nuclei concentration and the retrieved CDNC; between the MODIS retrieved and the SYRSOC-retrieved R_{eff} ; between the CLOUDNET-retrieved and the SYRSOC- retrieved LWC.

1. INTRODUCTION

The GAW atmospheric station of Mace Head in Ireland has deployed an impressive number of new instruments both in situ and remote sensing in the last five years. A k_a-band Doppler RADAR, a single-wavelength LIDAR, a temperature and humidity microwave radiometer (MWR) and an Aerodyne High Resolution Time of Flight Aerosol Mass Spectrometer (HR-ToF AMS) are, amongst the others, the most prominent improvement to the equipment already in place at the Mace Head supersite. An overview of multiple applications of different techniques to the remote sensing and in situ aerosol and cloud data is provided in the following sections. Section 2 shows an application of the Temporal Height Tracking algorithm [4,5,6] to backscatter and Doppler LIDAR returns to retrieve the vertical structure of the ABL during day and night. Section 3 describe the methodology to derive the LIDAR extinction and mass extinction based on the combination of in situ and LIDAR data. Section 4 shows different comparisons between SYRSOC and in-situ, satellite measurements and CLOUDNET retrievals of CDNC, R_{eff} and LWC, respectively, from liquid stratocumulus clouds.

2. ABL STRUCTURE

A comparative study of two different methods of retrieving the ABL structure has been performed by using vertical profiles of attenuated backscatter and Doppler velocity from a Halo Photonics pulsed Doppler LIDAR installed at Mace Head during the period 16-02-2012 to 28-03-2012 through the ACTRIS TNA framework (**A**erosols, **C**louds, and **T**race gases **R**esearch **I**nfra**S**tructure Network). The height of the ABL is an important parameter for many meteorological and air quality applications; however, this parameter must be carefully defined as different tracers and techniques can provide a different view of the ABL structure. For this study we have compared the heights retrieved from two definitions of the ABL: (i) the mixed-layer height, MLH, which is the top of the atmospheric region in constant contact with the surface through turbulent mixing [7]; (ii) the ABL as the top of the atmospheric layer where the friction and the convection generated at the surface influences directly the turbulent mixing which determines the homogeneous distribution of the aerosols [6]. While the first definition does not specify the nature of the tracers used to characterize the ABL and solely describes the MLH through its turbulent mixing, the second definition describes the ABL in terms of the aerosol distribution within the atmosphere as determined by friction, convection and advection. The THT is a 1-D (spatial) gradient and time-constrained technique to retrieve the ABL structure from any LIDAR returns. Because the THT works predominantly on the sharp changes along the profile it can be applied to different quantities like the aerosol concentration or the variance of the Doppler vertical velocity. THT retrieves two layers at each time

step: a Surface Mixed Layer (SML, lower layer) and a Decoupled Residual Layer (DRL, upper layer). The two layers are calculated by applying the THT to an *m*-by-*n* matrix (*m* = number of range gates; *n* = number of profiles) of logarithmic attenuated backscatter coefficient (β^{Att}) and turbulence (σ_{TKE}) from the Doppler LIDAR (see Eq.1). The SML retrieved from the β^{Att} and σ_{TKE} profiles are compared separately for day and night and for different air masses over Mace Head in Fig.1. The turbulence kinetic energy is defined as the unit mass mean kinetic energy of the turbulent vertical flow, that for this case applies to the fluctuations in the vertical component of the Doppler wind velocity (ω').

$$\beta^{Att} = \log(\beta) - 2\int_0^{\infty} \sigma dz \quad , \qquad \sigma_{TKE} = \frac{1}{2}(\omega')^2 \qquad (1)$$

2.1. Air mass classification

Three air masses characterized the period 16-02-2012 to 28-03-2012: maritime polar (*mP*), maritime tropical (*mT*) and continental polar (*cP*). Each comparison shows different characteristics based on the particular air mass (row-wise) and time of the day (column-wise). The top two panels show the *cP* air mass, the middle the *mP* and the bottom the *mT* (left: day; right: night). About 5% of the total SML data have been excluded from the comparison as the residuals were larger than 3 standard deviations. Compared to the *mT*, the SML data during both *cP* and *mP* distribute over a larger range of heights. During daytime the *cP* and *mP* SML are both ~160% of the *mT* values, the difference increases for the nocturnal retrievals when the *cP* and *mP* SML reach ~140% and 200% of the *mT* SML, respectively. Also the correlation coefficient is lower during *cP* and *mP*.

2.2. β^{Att} vs σ_{TKE}

The β^{Att}-retrieved SML values during *cP* are higher than the σ_{TKE}-retrieved ones during both day and night, especially at lower altitudes (<800 m) . The observed β^{Att}-σ_{TKE} relation must be interpreted in light of the general meteorological conditions during the *cP* air mass characterized by higher temperature and less clouds than the other periods. These conditions led to enhanced convection and turbulence dominating the MLH dynamics, the comparisons suggest that the level where the turbulence decays more abruptly is lower than the level where the aerosol concentration drops. Although observed during both day and night, this behaviour is more evident during day when convection dominates the dynamics . On the other hand, both *mP* and *mT* are characterized by moister air, lower temperature and more clouds. Especially the larger cloud cover led the two retrievals to converge more closely during the *mT* period: in fact both the backscatter and the turbulence profile undergo a dramatic change at the cloud base level. Generally, the comparison reveals a good agreement between σ_{TKE} and β^{Att} as tracers for the MLH. The comparison suggests also that clear-sky conditions would leave to more complex σ_{TKE} - β^{Att} relations.

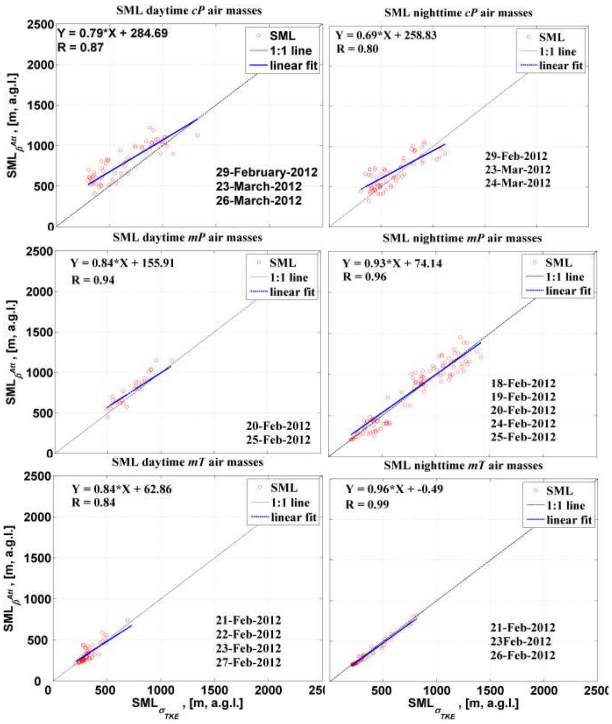

Figure 1. β^{Att} vs σ_{TKE} SML detection for different air masses and time of the day.

3. EXTINCTION AND MASS EXTINCTION

The retrieval of aerosol mass concentration from remote sensing and in-situ instrumentation has multiple applications in meteorology, air quality and boundary layer studies. The scientific community has tried to improve the accuracy of the estimated aerosol mass concentration for years. Unfortunately, ground-based remote sensing measurements alone can retrieve the profile of the mass load (***M***) only by assuming the density and the aerosol size distribution (ASD) of the aerosol population. These assumptions affect the retrieved value of ***M*** and increase its uncertainty. In order to retrieve an accurate profile of ***M*** using a backscatter or a Raman LIDAR with minimum assumptions in-situ information from co-located instrumentation are needed [8,9]. Here, we present a method to retrieve the aerosol mass concentration from synergistic remote sensing and in-situ measurements from LIDAR, MWR and TEOM (Tapered Element Oscillating Microbalance). The accuracy of the retrieved ***M*** depends on the accuracy of the extinction and on the Mass Extinction Efficiency (MEE). The Mass Extinction Efficiency (MEE) is the quantity that relates the LIDAR extinction ($\boldsymbol{\sigma}$) and ***M***, i.e. ratio of the total extinction in the column to the total column mass concentration of aerosols for any given ASD and any given wavelength at different heights, *z*:

$$M(z) = \frac{\sigma(z)}{MEE} \qquad (2)$$

The MEE is obtained after an initial calibration of the system in a well mixed boundary-layer and in homogeneous air mass conditions. The potential

temperature (TPOT) profile from the MWR provides information on the stability and mixing conditions of the atmospheric column above the sensor. Well-mixed conditions are selected based on the TPOT profile and an assumption of homogeneous conditions for aerosol concentration are taken for that time interval. The surface TEOM measurements of PM10 concentration are then used as a proxy for the mass $\boldsymbol{M}(z >= z_s)$ where z_s is the ground level altitude. Once the extinction is retrieved by inversion of the LIDAR signal, MEE can be calculated and used to calculate $\boldsymbol{M}(z)$ at any time during the homogeneous air mass conditions.

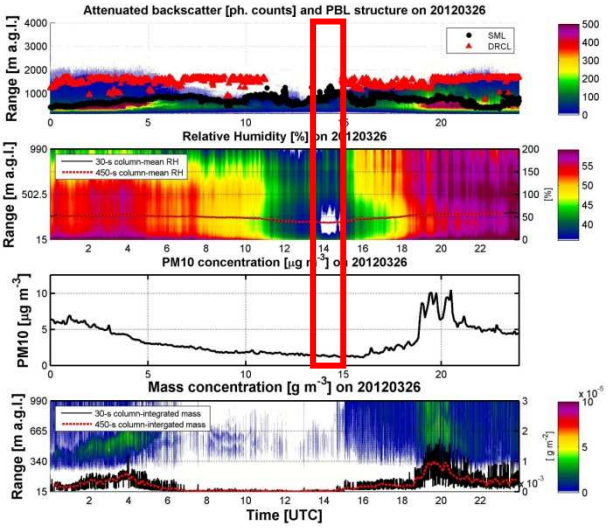

Figure 2. From top: THT-retrieved ABL heights from β^{Att} profiles; RH timeseries from the MWR; PM10 concentration; aerosol mass concentration.

Fig. 2 shows an example of application of this method to the LIDAR-RADAR-MWR and TEOM data to calculate $\boldsymbol{M}$ (bottom panel) for a clear-sky day in homogeneous continental air mass conditions at Mace Head. All information from top, middle-top and middle-bottom panels are used to constrain the method and reduce the uncertainty. The red highlighted area shows, in correspondence to the TPOT-based well-mixed conditions, the height of the SML (top), the RH value from the MWR (middle-top) and the PM10 concentration (middle-bottom).

4. LIQUID CLOUD MICROPHYSICS

SYRSOC (*SY*nergistic *R*emote *S*ensing *O*f *C*loud) is a multi-module technique capable to retrieve the three primary microphysical parameters from liquid clouds, i.e. CDNC, R_{eff} and LWC. In addition to the main microphysical variables, SYRSOC provides a number of parameters describing the cloud droplet spectral properties, the degree of cloud subadiabaticity, the Doppler velocity spectrum of droplets, the cloud optical depth and the cloud albedo. The 1064-nm wavelength CHM15K LIDAR, the RPG-HATPRO water vapour and oxygen microwave profiler and the 35-GHz K_a-band MIRA36 Doppler cloud RADAR installed at Mace Head are used to supply the input data to SYRSOC [1,2,3]. For the marine stratocumulus cloud detected over Mace Head during 11:00-16:00 UTC on the 10-Dec-2010, three comparisons have been performed between the main microphysical SYRSOC variables and, respectively, a poly-dispersed cloud condensation nuclei (CCN) counter for the CDNC, the MODIS satellite for the R_{eff} and CLOUDNET [10] for the LWC.

4.1. CDNC vs CCN

Fig. 3 shows the comparison between the CDNC and the surface-measured CCN at different supersaturation (*ss*) values, 0.1–0.25–0.5–0.75–1 %. The comparison relies on the fact that the boundary layer topped by the stratocumulus cloud was well mixed during the period 11:00-16:00 UTC. The agreement between the number of cloud droplets and activated nuclei confirms the robustness of the assumption. The CDNC-CCN comparison provides in this way an indirect estimate of the *ss* achieved within the cloud. As it is clear from the graph, during the first and last part of the cloud the ss was higher than during the central part.

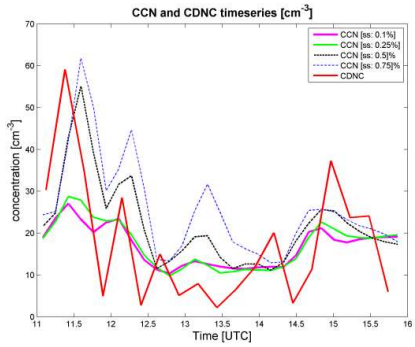

Figure 3. CDNC vs CCN at ss 0.1 –0.25 –0.5 –0.75 %.

4.2. SYRSOC vs MODIS: R_{eff}

L2 products of R_{eff} from AQUA Moderate-resolution Imaging Spectroradiometer (MODIS) satellites have been extracted for the overpasses containing the Mace Head station (53.33 N, 9.9 W).

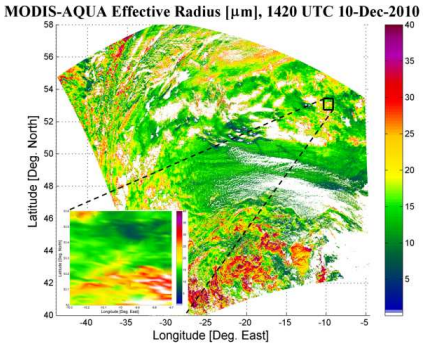

Figure 4. MODIS-AQUA R_{eff},14:20UTC overpass.

Fig. 4 shows the overpass for the marine cloud with highlighted 0.6×0.6-degrees box embedding the Mace Head geographical position. The box-averaged AQUA R_{eff} value is compared with the mean cloud top R_{eff} from SYRSOC. The 14:00–14:30UTC time interval has then been selected for SYRSOC to provide the mean R_{eff}. The satellite-retrieved R_{eff} was 16.2 µm and 17 µm was the mean upper layer SYRSOC-retrieved R_{eff}. Although

the error related to AQUA R_{eff} is much bigger than the one associated with SYRSOC, the comparison of "mean values" is encouraging providing very close R_{eff} retrievals.

4.3. SYRSOC vs CLOUDNET: *LWC*

The third comparison shows the relation and bias between the quasi-adiabatic LWC retrieved by SYRSOC and CLOUDNET for the 10-Dec-2010 case. CLOUDNET retrieves the LWC for profiles where the data have been diagnosed to be liquid water and where the liquid water path is available from the coincident MWR. Numerical model temperature and pressure values are used to estimate the theoretical adiabatic liquid water content gradient for each cloud base and the adiabatic liquid water content is then scaled so that its integral matches the MWR measurement. The so-retrieved liquid water content follows then a quasi-adiabatic profile. SYRSOC retrieves the LWC in two different ways, the subadiabatic and quasi-adiabatic.

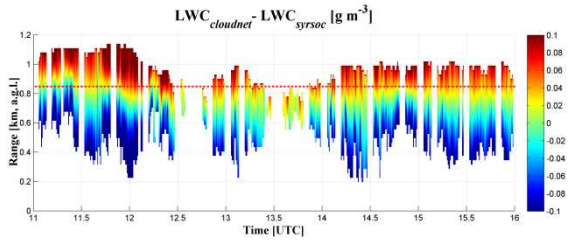

Figure 5. CLOUDNET-SYRSOC LWC

The subadiabatic LWC is a function of the CDNC, the RADAR reflectivity and the LIDAR extinction; the quasi-adiabatic LWC has a fixed slope and depends directly on the theoretical adiabatic liquid water content gradient, a constant subadiabatic factor (in the range 0-1) and the cloud thickness.

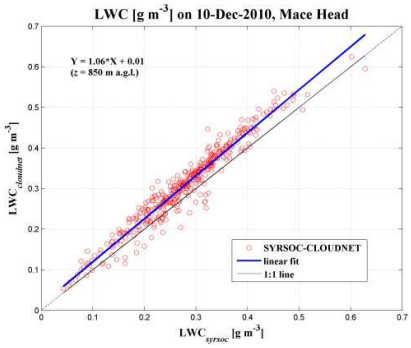

Figure 6. CLOUDNET vs SYRSOC at z= 850 m, a.g.l.

Only the quasi-adiabatic LWC from SYRSOC has been compared to the CLOUDNET LWC in Figs.5-6.The CLOUDNET-SYRSOC bias in Fig. 5 shows maximum departures of ±0.1 g m^{-3} (±14% of the max LWC), positive at the top and negative at the bottom of the cloud. The discrepancy between the two shows that CLOUDNET has a steeper LWC slope through the cloud. Fig. 6 shows for the 850-m altitude slice the comparison between the two retrievals in a scatter plot, showing more clearly the 0.1-g m^{-3} positive bias in the top region of the cloud.

4.4. SUMMARY

The WMO/GAW Mace Head station is a state-of-the-art reference in different fields of atmospheric science. The presented results open to new applications and studies like the investigation of the turbulence as a proxy for the ABL structure. Also the accurate retrieval of the mass extinction is paramount in order to combine the information from the aerosol load and the cloud microphysics retrieved by SYRSOC.

Acknowledgments: We kindly acknowledge the European Community - Research Infrastructure Action under the FP7 "Capacities" specific programme for Integrating Activities, ACTRIS Grant Agreement no. 262254 for the support to the project: Investigation of marine boundary layer and clouds with remote sensing instruments at Mace Head.

5. REFERENCES

1. Martucci, G. and O'Dowd, C. D. 2011: Ground-based retrieval of continental and marine warm cloud microphysics, *Atmos. Meas. Tech*., **4**, 2749-2765

2. Ovadnevaite, J., D. Ceburnis, et al. (2011). Primary marine organic aerosol: A dichotomy of low hygroscopicity and high CCN activity, *Geophys. Res. Lett.*, **38**, L21806

3. Martucci, G., J. Ovadnevaite, et al. (2012): Impact of volcanic ash plume aerosol on cloud microphysics. *Atmospheric Environment*, **48C**, 205-218.

4. Martucci, G., Milroy, C., O'Dowd, C.D. (2010). Detection of Cloud Base Height Using Jenoptik CHM15K and Vaisala CL31 Ceilometers. *J. Atmos. Oceanic Technol*. Vol. **27**, No. 2, 305–318.

5. Haeffelin, M., F. Angelini, et al. (2011). Evaluation of mixing depth retrievals from automatic profiling lidars and ceilometers in view of future integrated networks in Europe. *Boundary-Layer Meteorology*, DOI 10.1007/s10546-011-9643-z

6. Milroy, C., G. Martucci, et al. (2012). An Assessment of Pseudo-Operational Ground-Based Light Detection and Ranging Sensors to Determine the Boundary-Layer Structure in the Coastal Atmosphere. *Advances in Meteorology*, **2012**, ID 929080, 18 pages. doi:10.1155/2012/929080

7. White, J. M., J. F. Bowers et al. (2009). Importance of using observations of mixing depths in order to avoid large prediction errors by a transport and dispersion model. *Journal of Atmospheric and Oceanic Technology*, **26**, pp. 22–32.

8. Lewandowski, P. A., Eichinger, et al. (2010). Vertical distribution of aerosols in the vicinity of Mexico City during MILAGRO-2006 Campaign, *Atmos. Chem. Phys.*, **10**, 1017-1030

9. Hervo, M., Quennehen, et al. (2012). Physical and optical properties of 2010 Eyjafjallajökull volcanic eruption aerosol: ground-based, Lidar and airborne measurements in France, *Atmos. Chem. Phys*., **12**, 1721-1736.

10. Illingworth, A.J., R.J. Hogan, et al. (2007). Cloudnet - continuous evaluation of cloud profiles in seven operational models using ground-based observations. *Bull. Amer. Meteor. Soc.*, **88**, 6, 883-898.